

## The effect of cavitation on the natural frequencies of a hydrofoil

Oscar de la Torre  
UPC-CDIF

Xavier Escaler  
UPC-CDIF

Eduard Egusquiza  
UPC-CDIF

Matthieu Dreyer  
LMH-EPFL

Mohamed Farhat  
LMH-EPFL

### SUMMARY

The objective of the present paper is to show the effect of cavitation on the natural frequencies of a NACA0009 hydrofoil. The existence of large portions of the hydrofoil surface covered by vapor is expected to reduce the added mass effects of the surrounding flowing water. For that, a specific excitation and measuring system based on piezoelectric patches has been developed and validated. With this experimental setup, the three first natural frequencies of an aluminum NACA 0009 truncated hydrofoil have been determined in various conditions. The hydrofoil has been tested with partial cavitation and with supercavitation at 14 m/s and two incidence angles of 1° and 2°. Analogous tests have been carried out with the hydrofoil in air and surrounded by still water. The comparison of all the results has confirmed the significant role that cavitation plays in the modal response of the hydrofoil.

### INTRODUCTION

The natural frequencies of a structure submerged in water experience a significant decrease due to the added mass effect [1, 2]. In the field of hydraulic machinery, the frequency reduction affecting runners/impellers should be estimated a priori to foresee resonance problems during operation. For instance, recent investigations demonstrate that the frequency reduction ratio depends on the mode shape [3]. However, no attention has been given up to now to the possible influence of large scale vapor/gas cavities or pockets surrounding the structure under cavitating flows. Only the cases in still fluid of partially submerged bodies have been investigated. For instance, Lindholm et al. carried out in 1965 the modal analysis of submerged beams at various depths [4]. Therefore, in the present work the effects of partial cavitation and supercavitation on the natural frequencies of a hydrofoil have been experimentally investigated in a high speed cavitation tunnel.

### EXPERIMENTAL SET UP

A series of measurements have been carried out with an aluminum NACA0009 hydrofoil in different situations at the LMH-EPFL High Speed Cavitation Tunnel [5] shown in Figure 1 in order to determine its first natural frequencies.

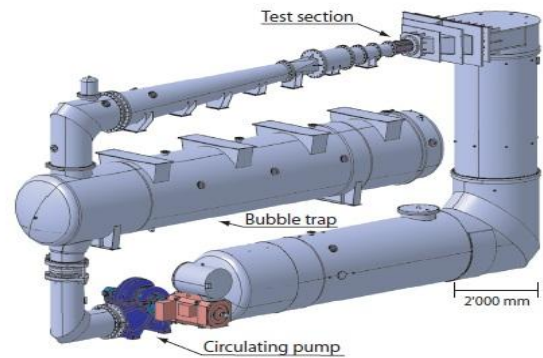


Figure 1: LMH High speed cavitation tunnel

The profile has a chord of 100 mm and a span of 150 mm. Its trailing edge is truncated at 90% of the chord leaving a trailing edge thickness of 3.22 mm. The current paper studies the effect on the first and second bending natural frequencies ( $f_1$  and  $f_3$ ) and on the first torsion natural frequency ( $f_2$ ) previously identified and determined by Ausoni *et al.* [6]. Several scenarios have been tested to clarify the relative importance of certain variables on the natural frequencies of the hydrofoil. In particular, the different hydrodynamic conditions considered for the experiments are the following ones:

- Hydrofoil surrounded by air.
- Hydrofoil lower surface wetted with still water.
- Hydrofoil completely submerged in still water.
- Hydrofoil completely submerged in flowing water and with attached partial cavitation.
- Hydrofoil completely submerged in flowing water and surrounded by supercavitation mainly on the suction side.

The tests with cavitation conditions have been carried out at 14 m/s and for two incidence angles of 1° and 2°.

A specific set-up and procedure has been developed to carry out the experimental modal analysis. In order to excite the profile

and measure its response, a new excitation system has been designed and proved to be able to excite the hydrofoil when mounted on the cavitation tunnel test section full of water and, hence, without external access. A preliminary work, which gave promising results, was done in laboratory conditions on metallic plates to evaluate the suitability of using piezoelectric patches. The piezoelectric technology was chosen due to its capability to be used onboard either as an excitation system or as a sensing device. This previous work permitted to select the adequate piezoelectric patch and voltage input capable of generating a large enough excitation force that could provoke a significant response. The amplitude of the response had to be sufficiently high to be measured in such a noisy environment as a cavitation tunnel under flow conditions. On the other hand, the patch used as a sensor showed a good measuring characteristics and it was proven to be as reliably as an accelerometer. Since piezoelectric devices are present in a wide variety of configurations, flexible piezoelectric patches were selected due to their adaptability to curved surfaces. They were integrated on the hydrofoil surface without altering the hydrodynamic geometry and therefore the flow field was not affected with their use. In particular, two piezoelectric patches (61mm x 35mm x 0.5mm) were embedded on the upper surface of the hydrofoil (Figure 2). Their mounting required a precise mechanization and fixation work. Special attention was given to their optimal location which depends on the mode to be excited and investigated. In the current work, a compromise had to be reached to excite bending and torsion modes. During the tests the patch closer to the leading edge was used as an exciter and the patch closer to the trailing edge as a sensor.

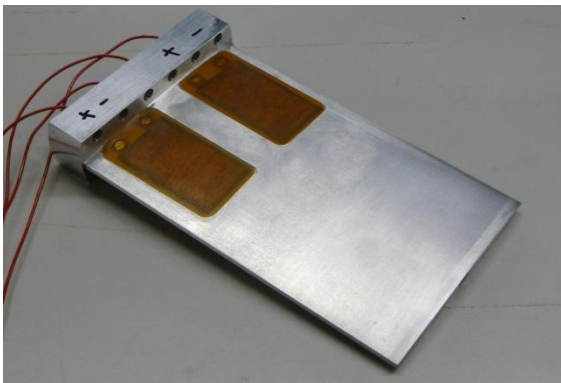


Figure 2: Piezoelectric patches mounted on the NACA0009 profile.

In order to excite the profile a sinusoidal chirp signal was fed to the leading edge patch. This chirp was chosen to sweep frequency bands containing the expected natural frequencies. Then, the detection of the amplified response due to the resonances permitted to identify the natural frequencies. In Figure 3 and example of the excitation signal (on the top) and of the simultaneous response signal (on the bottom) during one of the tests are shown (the horizontal axis indicates time). It is observed how when the frequency of the excitation coincides with a natural frequency corresponding to the 1<sup>st</sup> bending and the torsion modes of vibration the amplitudes of the measured signal are significantly amplified and can be well identified.

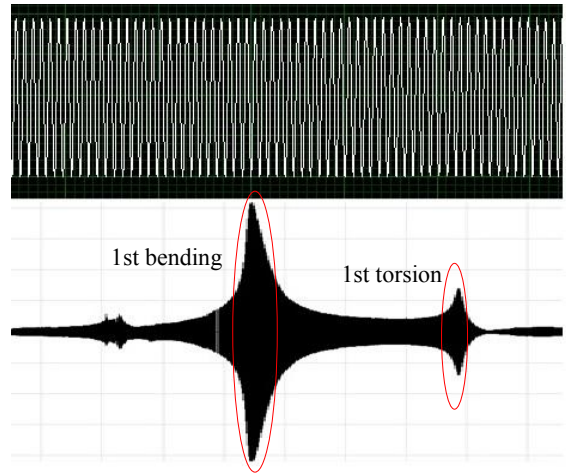


Figure 3: Examples of excitation signal and response signal.

## METHODOLOGY

The previous results shown in Figure 3 correspond to static air conditions which are very clear, but under flow conditions the induced noise difficults the identification of the resonances. Therefore, a specific signal processing method was developed to remove other sources of noise and to enhance the correlation between the forced excitation and its response. Once the signals are obtained, the Cross Power Spectrum (CPS) between segments of the input and the response signals is calculated. As the input signal (chirp) varies its frequency linearly, sliding filters and windows have to be used to limit the frequency band where the CPS is applied at a particular time and to reduce noise. Despite of this procedure, the partial cavitation cases presented difficulties to find a clear frequency with amplification from the CPS. In such conditions, a curve fitting method was used to estimate the resonance. Besides, a Joint Time Frequency Analysis (JTFA) was also performed to validate the method and analogous results were obtained. This JTFA was based on the short time Fourier transform (STFT) which is one of the most extended methods to analyze a time-varying signal. Basically, with this method the response signal is cutted into overlapped data blocks by means of sliding windows and then the fast Fourier transform (FFT) is applied to each data block. The results are plotted in a 3D graph with the horizontal axis indicating time, the vertical axis indicating frequency and the z-axis indicating the amplitude with a color scale. An example is shown in Figure 4 for the response of the 1<sup>st</sup> bending mode measured in air conditions.

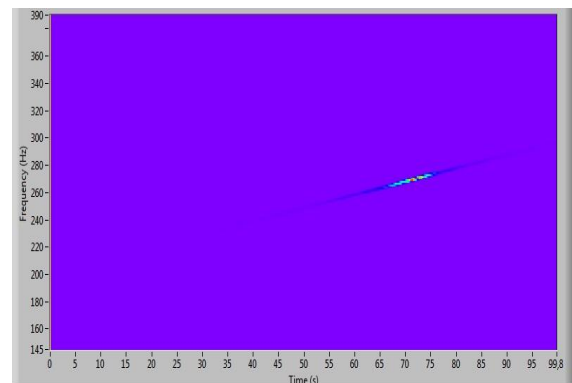


Figure 4: Time-frequency spectrogram of the 1<sup>st</sup> bending mode blade resonance in air.

## RESULTS AND DISCUSSION

As it has been said before, a series of experimental modal tests were performed with the hydrofoil under different boundary conditions. Visual inspections of such conditions were carried out. As an example, two photographs of the flow field observed from a transparent lateral window of the tunnel test section are shown in figures 5 and 6. In Figure 5 the suction side partial attached cavity reaching approximately the 44% of the chord for 1° incidence angle is shown. For 2° incidence the length of the cavity reached approximately the 53% of the chord. In Figure 6, the supercavity generated at a similar flow speed and 2° is shown. In both 1° and 2° cases, it has to be mentioned that the supercavitation mainly took place on the hydrofoil suction side and only few spots of cavitation were present on the pressure side.

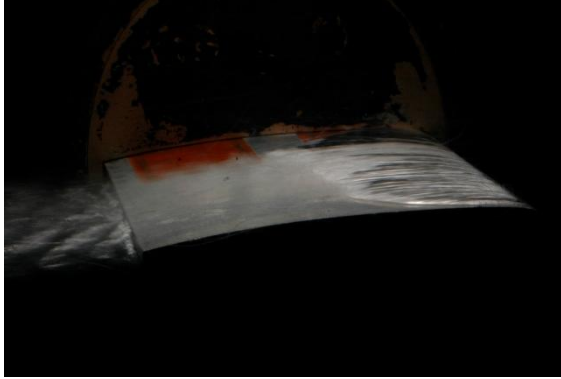


Figure 5: Partial cavitation at 14 m/s and 1°.



Figure 6: Supercavitation at 14 m/s and 2°.

Tables 1, 2 and 3 summarize the results obtained in terms of natural frequencies for the three first mode shapes in all the cases which correspond to static conditions (no flow), cavitation conditions at 1° and cavitation conditions at 2° incidence angles, respectively. In order to compare these results, the values of the frequencies measured in air are taken as a reference. So, the effect of the added mass on the natural frequencies is quantified by the use of the so-called frequency reduction ratio (FRR), which has been defined by Equation 1:

$$FRR_{i,j} = \frac{|f_{i,j} - f_{air,j}|}{f_{air,j}} \quad (1)$$

where  $f_{i,j}$  is the natural frequency of the hydrofoil for the  $j$  mode and under  $i$  conditions and  $f_{air,j}$  is the natural frequency for the  $j$  mode in air.

|             | $f1$ (Hz) | $f2$ (Hz) | $f3$ (Hz) |
|-------------|-----------|-----------|-----------|
| Air         | 270.2     | 1018.6    | 1671.0    |
| Half Wetted | 163.0     | 755.0     | 1113.6    |
| Still Water | 130.2     | 614.8     | 886.0     |

Table 1: Natural frequencies in static conditions (no flow).

| $I^\circ$                           | $f1$ (Hz) | $f2$ (Hz) | $f3$ (Hz) |
|-------------------------------------|-----------|-----------|-----------|
| Partial Cavitation ( $l/c = 0,44$ ) | 135.4     | 677.6     | 996.8     |
| Supercavitation                     | 248.7     | 918.4     | 1460      |

Table 2: Natural frequencies for partial cavitation and supercavitation cases at 14 m/s and 1°.

| 2°                                | $f1$ (Hz) | $f2$ (Hz) | $f3$ (Hz) |
|-----------------------------------|-----------|-----------|-----------|
| Partial Cavitation ( $l/c=0,53$ ) | 146.2     | 696.3     | 989.8     |
| Supercavitation                   | 235.2     | 879.9     | 1402.3    |

Table 3: Natural frequencies for partial cavitation and supercavitation cases at 14 m/s and 1°.

In figures 7 and 8, the FRR's calculated with the values of the natural frequencies presented in the corresponding tables are plotted for 1° and for 2° incidence angles, respectively. For a correct interpretation of the results it has to be reminded that the higher the FRR value, the higher the added mass effect. Consequently, it is confirmed that the maximum added mass effect takes place when the hydrofoil is submerged in still water. In this case, the natural frequencies are reduced between the 40% and 52% depending on the mode shape.

As can be confirmed from Table 1, the natural frequencies when the hydrofoil is Half Wetted are not exactly located half way between the Air and Still Water cases as could be expected. Besides, the frequency shift is mode dependent and the FRR is higher for lower order mode shapes as already found by [3].

Comparing Partial Cavitation results with Still Water ones plotted on figures 7 and 8, it is observed how the order of importance of the added mass effect is maintained among the different mode shapes.

From the comparison of Supercavitation results at both incidence angles, a difference up to 5% is observed with larger effects for the case of 2°.

Comparing Supercavitation and Partial Cavitation results for both incidence angles, it is observed that there is not a linear relation between the area of the hydrofoil covered by the vapor content of the cavitation and the frequency shift. This fact may indicate that several other variables can have a role in this phenomenon such as the void fraction, the mode shape deformation and others.

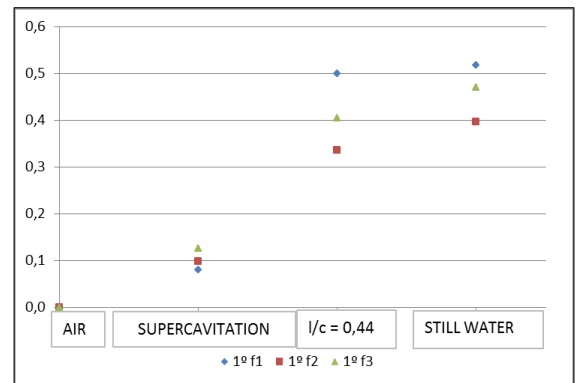


Figure 7: FRR for different scenarios at 1°.

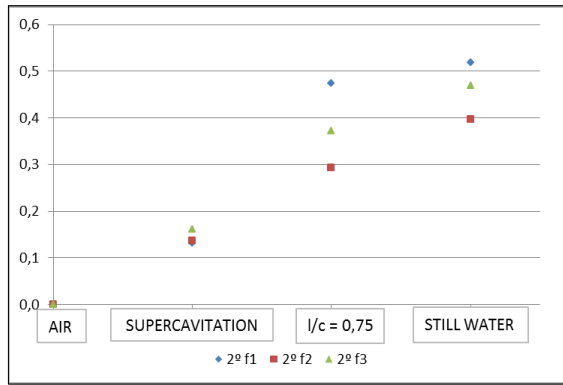


Figure 8: FRR for different scenarios at 2°.

But in general terms, it is confirmed that the results are consistent and that the trends of the FRR values are analogous for all the modes at both incidences angles.

## CONCLUSION

An experimental investigation to determine the effects on the natural frequencies of a hydrofoil submerged in a cavitating flow has been presented.

A specific system based on piezoelectric patches has been developed and used to perform the experimental modal analysis under flowing conditions without altering the flow field.

The three first natural frequencies of the hydrofoil have been found under partial cavitation and supercavitation conditions. These results have also been compared to the frequencies found in static fluid conditions comprising air, water and a mixture of both.

It has been confirmed that the presence of a large scale attached cavitation form on the hydrofoil surface results in a significant increase of any of its three first natural frequencies with respect to the still water case. Moreover, such increase is mode dependent. Therefore, the added mass effect is reduced.

Moreover, it has been also been found that the area of the attached cavity or the static air in contact with the hydrofoil surface is not the unique parameter that determines the reduction of the added mass effect. Hence, for both static and dynamic cases,

several more variables might also play a role in the final added mass effect.

## ACKNOWLEDGMENTS

The present investigation is part of the work carried out for Hydrodyna Phase II research project. The authors would like to acknowledge all the partners of the project (ANDRITZ Hydro, ALSTOM Hydro, VOITH Hydro, LMH-EPFL and CDIF-UPC) for their collaboration.

## NOMENCLATURE

|       |   |
|-------|---|
| $f_1$ | natural frequency of the 1 <sup>st</sup> bending mode                 |
| $f_2$ | natural frequency of the torsion mode                                 |
| $f_3$ | natural frequency of the 2 <sup>nd</sup> bending mode                 |
| CPS   | Cross Power Spectrum  |
| FFT   | Fast Fourier Transform  |
| FRR   | Frequency reduction ratio = $\frac{ f_{i,j} - f_{air,j} }{f_{air,j}}$ |
| JTFA  | Joint Time Frequency Analysis   |
| STFT  | Short Time Fourier Transform  |

## REFERENCES

- [1] Brennen, C., 1982, *A review of added mass and fluid inertial forces*. Naval Civil Engineering Laboratory.
- [2] Blevins, R. D., 1979, *Formulas for natural frequency and mode shape*. Krieger, Malabar..
- [3] Yadykin, Y., Tenetov, V., Levin, D., 2003, *The added mass of a flexible plate oscillating in a fluid*. Journal of fluids and structures 17, 115-123.
- [4] Lindholm, U.S., Kana, D.D., Chu, W.-C., Abramson, H.N., 1965, *Elastic vibration characteristics of cantilever plates in water*. Journal of Ship Research 9, 11-22.
- [5] Avellan, F., Henry, P., Ryhming, I.L., 1987, *A new high speed cavitation tunnel*. ASME Winter Annual Meeting, Boston 57, 49-60.
- [6] Ausoni, Ph., Farhat, M., Escaler, X., Egusquiza, E., Avellan, F., 2007, *Cavitation influence on Von Kármán vortex shedding and induced hydrofoils vibrations*. Journal of fluids engineering, Volume 129, Issue 8, 966 (8 pages)